Available online at www.sciencedirect.com
ScienceDirect
Ceramics International 33 (2007) 1389–1393
CERAMICS INTERNATIONAL
www.elsevier.com/locate/ceramint

Short communication

Microstructures and microwave dielectric properties of Li_2O–Nb_2O_5–ZrO_2 ceramics

Chun-An Lu [a], Pang Lin [a], Sea-Fue Wang [b,*]

[a] Department of Materials Science and Engineering, National Chiao Tung University, Hsinchu, Taiwan, ROC
[b] Department of Materials and Mineral Resources Engineering, National Taipei University of Technology, 1, Section 3, Chung-Hsiao East Road, Taipei, Taiwan, ROC

Received 27 November 2005; received in revised form 29 March 2006; accepted 29 April 2006
Available online 15 September 2006

Abstract

Solid solution of $Li_{1-4y-x}Zr_{y+4x}Nb_{1-3x}O_3$ system is a new non-stoichiometric compound with orthorhombic perovskite structure. In this study, the effects of the calcination and the sintering temperatures on the microstructural evolution and microwave dielectric properties of $Li_{1-4y-x}Zr_{y+4x}Nb_{1-3x}O_3$ ceramics were performed. Dense $Li_{0.774}Zr_{0.057}NbO_3$ ceramics can be obtained at the sintering temperature of 1150 °C. $Li_{0.774}Zr_{0.057}NbO_3$ phase exists as the main phase with the existence of a minor $LiNb_3O_8$ phase. Typical microwave dielectric properties for dense $Li_{0.774}Zr_{0.057}NbO_3$ ceramics are as followed: $\varepsilon_r \approx 39$, $Q \times f \approx 4500$, and $\tau_f = -16.6$ ppm/°C, measured at 6 GHz.
© 2006 Elsevier Ltd and Techna Group S.r.l. All rights reserved.

Keywords: Microwave properties; Densification; Microstructural evolution; Li_2O–Nb_2O_3–ZrO_2 system

1. Introduction

The recent rapid expansion of telecommunication systems demands dielectric resonators (DRs) as basic components for designing filters and oscillators. Now, dielectric ceramics for use in resonators at microwave frequency have been paid increasing attention due to the fast growth of mobile communication systems such as cellular phone, global positioning systems and personal communication system. For the applications in microwave devices, a high dielectric constant ($\varepsilon > 20$), a high dielectric loss quality ($Q > 2000$), and a near zero temperature coefficient of resonant frequency (0–10 ppm/°C) are required. High dielectric constant makes possible to reduce the size of the material by factor of $1/\varepsilon_r^{1/2}$ so that size of the circuit can be reduced considerably. The high Q values enable low insertion loss and low bandwidth of the resonance frequency, which is required for achieving high frequency selectivity and stability in the microwave transmitter components.

Recently, dielectric material often required to be co-fired with high conductivity electrode such as Ag and Cu in order to minimize the microwave absorption loss or to form a multilayer structure to increase the volume efficiency. However, the sintering temperatures of common dielectric ceramics are in the range between 1200 and 1500 °C, which is much higher than the melting temperature of Ag (961 °C) or Cu (1064 °C). For instance, the sintering temperatures of BaO–Nd_2O_3–TiO_2–Nb_2O_5, $Ba_{6-x}Ln_{8+2x/3}Ti_{18}O_{54}$ and $(Zr,Sn)TiO_4$ systems are around 1325, 1350 and 1400 °C, respectively [1–3]. There is considerable interest in the development of new materials with low sintering temperatures. One way involved is the investigations of the glass-forming additives on the properties of established microwave materials. For instance, the BaO–La_2O_3–$4.7TiO_2$ ceramic with the addition of 20 wt.% PbO–B_2O_3–SiO_2 aids can reduce the sintering temperature down to 900 °C, but the microwave properties were degraded [4]. Another way is the use of the new material systems with lower sintering temperatures [5]. For instance, the sintering temperature of $Bi_{12}MO_{20-\delta}$ (M = Si, Ge, Ti, Pb, Mn, $B_{1/2}P_{1/2}$), TiO_2–TeO_2, Bi_2O_3–ZnO–Nb_2O_5, and Li_2O–Nb_2O_5–MO_2 (M = Ti, Zr) are around 680–850, 720, 950, and 1150 °C, respectively [6–8].

Among the low sintering compounds, Villafuerte-Castrejon et al. [9] were first to report the solid solutions of $Li_{1-4y-x}Zr_{y+4x}Nb_{1-3x}O_3$ system, for which $y = 0.057$ and $0 < x < 0.15$ system. This new system is a non-stoichiometric compound with orthorhombic perovskite structure which is fairly close to $LiNbO_3$. The structure is based on a complete

* Corresponding author. Fax: +886 2 2731 7185.
E-mail address: seafuewang@yahoo.com (S.-F. Wang).

0272-8842/$32.00 © 2006 Elsevier Ltd and Techna Group S.r.l. All rights reserved.
doi:10.1016/j.ceramint.2006.04.013

three-dimensional array of corner-sharing NbO_6 octahedra. Up to now, there have been no reports on their microwave dielectric properties yet. In this study, the solid solution of $Li_{0.774}Zr_{0.057}NbO_3$ ($y = 0.057$, $x = 0$) was used throughout. The effects of the calcination and the sintering temperatures on the microstructural evolution and microwave dielectric properties of $Li_{0.774}Zr_{0.057}NbO_3$ are investigated, and the relationships among them are discussed.

2. Experimental procedure

Ceramic samples were prepared through the conventional solid-state reaction of reagent-grade Li_2CO_3 (99.9%), Nb_2O_5 (99.8%) and ZrO_2 (99%). The powders were mixed in methyl alcohol solution using polyethylene jars and zirconia media for 8 h. After drying, the powders were preheated at 700 °C to remove carbon dioxide at 700 °C, and followed by calcining at 1000, 1050, 1100 and 1150 °C for 10 h. After calculation, the powders were remilled in methyl alcohol for 12 h. The powders have particle size (d_{50}) of ≈0.34 μm measured by light scattering (Zeta 1000) and surface area of ≈2.3 m^2/g from B.E.T. method. The granulated powders with a PVA binder were then dry-pressed under 1 ton to form pellets (9 mm in diameter). They were then de-bindered at 550 °C for 4 h and subsequently sintered in air at 950, 1000, 1050, 1100 and 1150 °C for 1 h, with a heating rate of 10 °C/min. Differential thermal analysis (DTA) was performed in a Pt crucible with a heating rate of 10 °C/min using a Perkin-Elmer Calorimeter (Series 1700 DTA), on mixtures to evaluate the melting reactions.

The densified cylindrical samples were polished to have an exact thickness of 5 mm for the measurements of microwave properties. Bulk densities of the sintered samples were measured using the Archimedes method with de-ionized water. Phase identification on the calcined powders as well as the sintered bulk ceramics were performed using X-ray diffraction (XRD, Simens D5000). The microstructures of the sintered samples were observed using scanning electron microscopy (SEM, JEOL 6500F). The grain size was determined from SEM micrographs by linear intercept method. The sintered samples were further inspected by transmission electron microscopy (Model Tecnai 20 by Philips), to understand the distribution of various species. The dielectric constant (ε_r) and quality factor ($Q \times f$) were evaluated, based on the cylindrical cavity method (cavity 1005CIRC and software CAVITY, Damaskos Inc.), using a HP 8722D network analyzer. Detailed measurement procedures have been described elsewhere [10]. The temperature coefficient of resonant frequency (τ_f) was measured within the range from 25 to 80 °C. The τ_f was defined by $(f_T - f_{25})/f_{25}(T - 25\,°C)$ in Damaskos cavity.

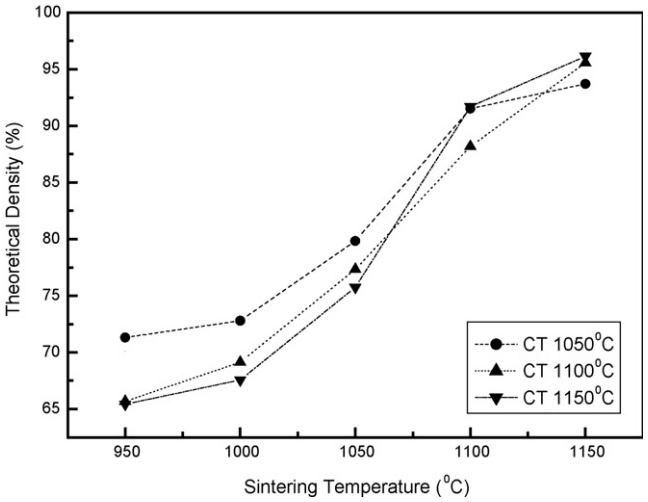

Fig. 2. Densities of the $Li_{0.774}Zr_{0.057}NbO_3$ ceramics sintered at different temperatures, for the powders prepared at different calcinations temperatures.

3. Results and discussion

XRD patterns for the $Li_{0.774}Zr_{0.057}NbO_3$ powders calcined at different temperatures for 10 h are shown in Fig. 1. For the

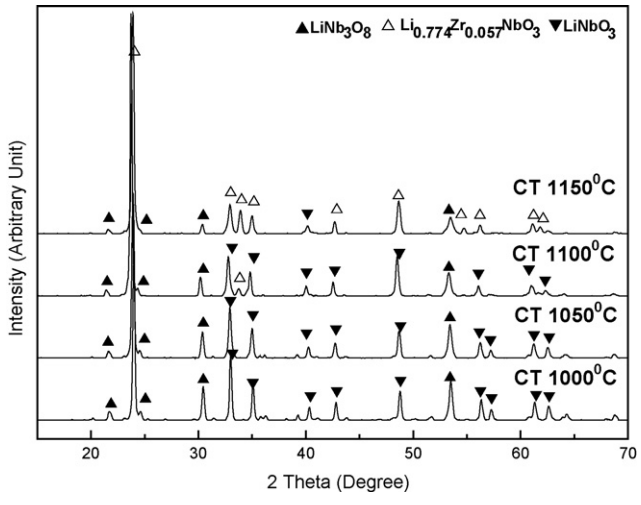

Fig. 1. XRD patterns of $Li_{0.774}Zr_{0.057}NbO_3$ powders with different calcination temperatures.

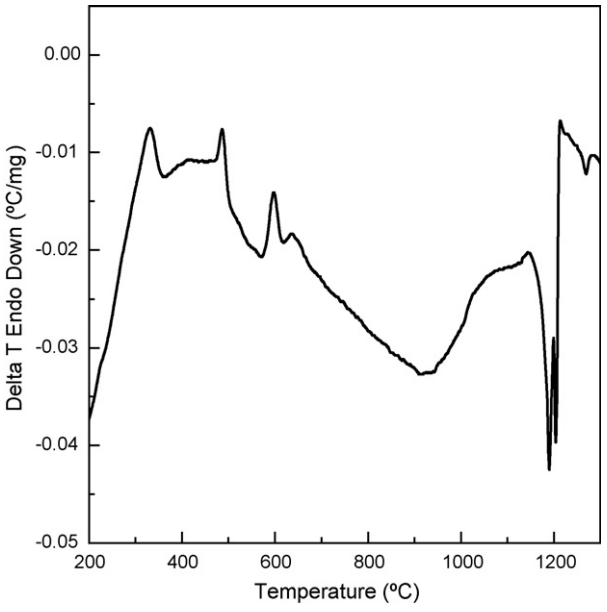

Fig. 3. DTA results of $Li_{0.774}Zr_{0.057}NbO_3$ powder.

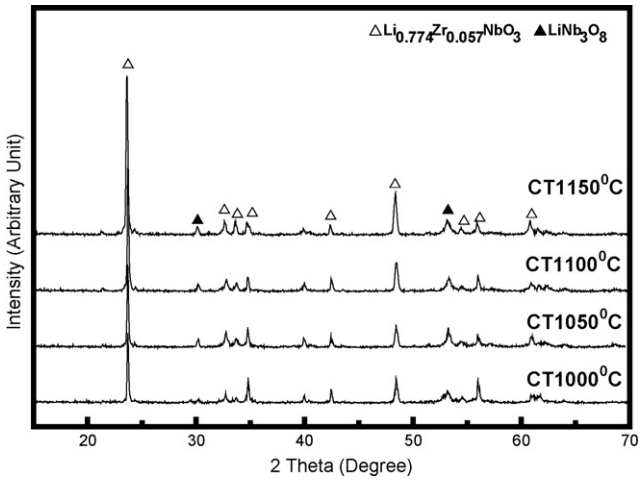

Fig. 4. XRD patterns of $Li_{0.774}Zr_{0.057}NbO_3$ ceramics, with different calcination temperatures, sintered at 1150 °C.

powders calcined at 1000 and 1050 °C, $LiNbO_3$ and $LiNb_3O_8$ phases co-exist. Peaks attributed to ZrO_2 are not observed in the XRD patterns due to its small quantity. As the calcination temperature reaches 1100 °C, $Li_{0.774}Zr_{0.057}NbO_3$ phase starts to form. The peak intensities of $LiNb_3O_8$ and $LiNbO_3$ phases continue to decrease as the calcination temperature increases. This is due to the formation of $Li_{0.774}Zr_{0.057}NbO_3$ solid solution that induces the $LiNbO_3$ phase to release Li content, which then reacts with $LiNb_3O_8$ and ZrO_2 to generate more $Li_{0.774}Zr_{0.057}NbO_3$. Well-crystallized $Li_{0.774}Zr_{0.057}NbO_3$ phase with orthorhombic structure was obtained at 1150 °C accompanied with minor $LiNb_3O_8$ and $LiNbO_3$ phases.

The theoretical sintered densities of $Li_{0.774}Zr_{0.057}NbO_3$ ceramics sintered at different temperatures are indicated in Fig. 2. The curves in the figure correspond to the powders previously calcined at 1050, 1100, and 1150 °C, respectively. The results show that over 95% theoretical densities can be obtained when the sintering temperature reaches 1150 °C, regardless the previous calcination temperatures. Sintering temperature beyond 1150 °C was not pursued due to the fact that a liquid phase formation at ≈1190 °C, according to the DTA result (Fig. 3). Fig. 4 gives the XRD patterns of $Li_{0.774}Zr_{0.057}NbO_3$ ceramics prepared from the powders calcined at different temperatures and subsequently sintered at 1150 °C. In all cases, $Li_{0.774}Zr_{0.057}NbO_3$ phase exists as the main phase with the existence of a minor $LiNb_3O_8$ phase, which may result from the loss of Li by evaporation.

The SEM microstructures of ceramics prepared from various calcination and sintering temperatures are shown in Fig. 5. It seems that the microstructures are closely correlated to the

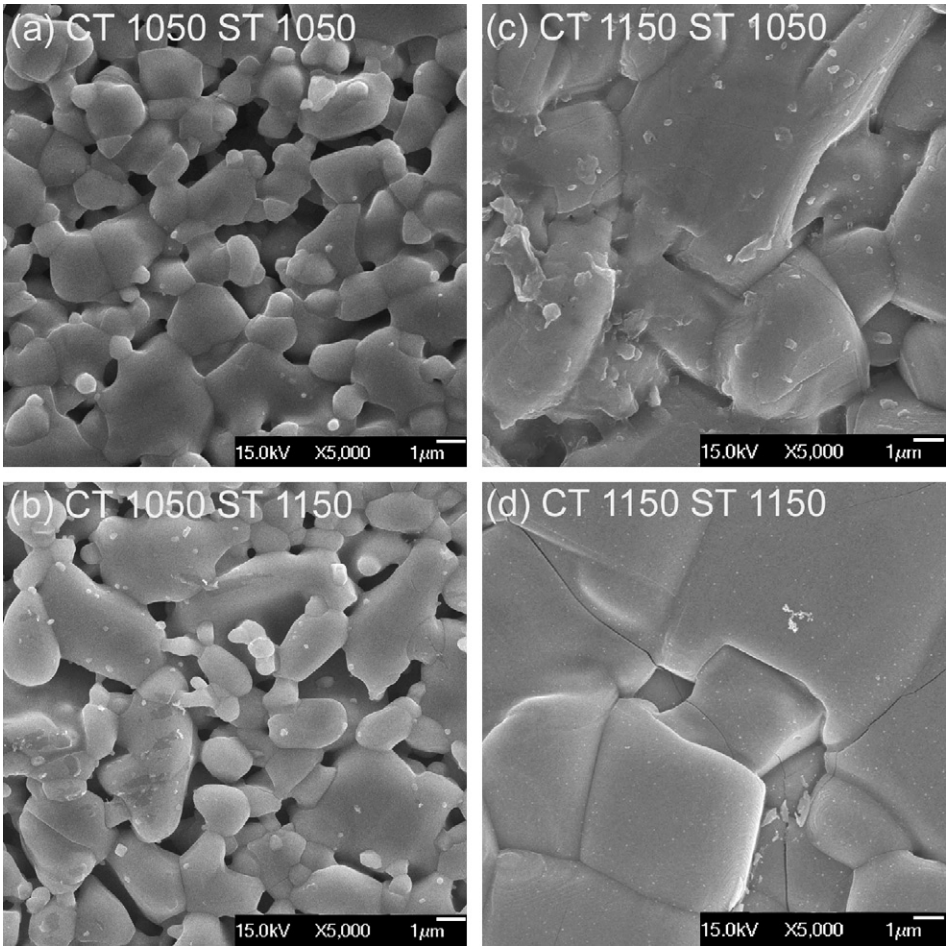

Fig. 5. SEM micrographs of $Li_{0.774}Zr_{0.057}NbO_3$ ceramics prepared from different calcination temperatures (CT) and different sintered temperatures (ST): (a) CT1050 °C/ST1050 °C, (b) CT1050 °C/ST1150 °C, (c) CT1150 °C/ST1050 °C, and (d) CT1150 °C/ST1150 °C.

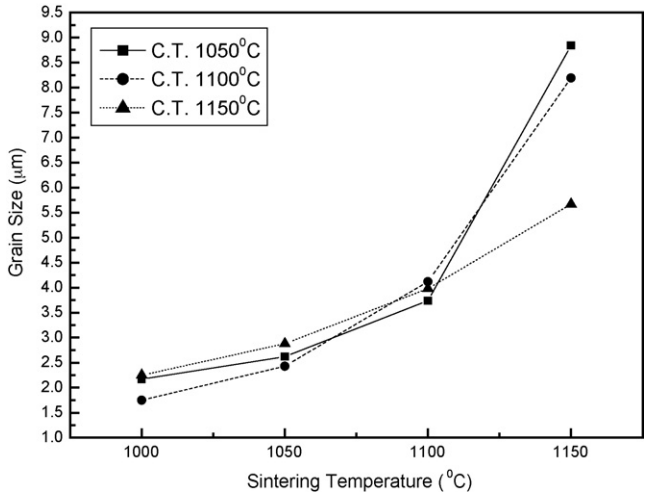

Fig. 6. Grain sizes of $Li_{0.774}Zr_{0.057}NbO_3$ ceramics with different calcination temperatures as a function of sintering temperature.

sintering temperature but not the calcination temperature. Generally, the ceramics of $Li_{0.774}Zr_{0.057}NbO_3$ were porous when sintered at 1050 °C. As the sintering temperature increased to 1150 °C, dense $Li_{0.774}Zr_{0.057}NbO_3$ ceramics were obtained accompanied with a significant grain growth. Fig. 6 shows the average grain size of $Li_{0.774}Zr_{0.057}NbO_3$ ceramics at different sintering temperatures. The grain sizes of $Li_{0.774}Zr_{0.057}NbO_3$ ceramics increase gradually from ≈2 to ≈4 μm as the sintering temperature increased from 1000 to 1100 °C, in spite of the different calcination temperatures. Significant grain growth was observed for sintering temperature above 1150 °C, at which the grain sizes are in the range of 5–9 μm.

In order to reveal the detailed information of the structure, $Li_{0.774}Zr_{0.057}NbO_3$ ceramic was examined by TEM and the result is shown in Fig. 7. The areas A and B in the bright field image had a similar diffraction pattern, but discrepancy in the d-space and the face angle. The electron diffraction patterns identified by d-space are corresponding to the $Li_{0.774}Zr_{0.057}NbO_3$ phase. The area *C* was identified as $LiNb_3O_8$ phase. These results are coincidence with the XRD results discussed above. In the bright field, it exhibited the growing lath crystal that is derived from the grain coarsing through the surface diffusion and boundary diffusion. Furthermore, it is found that the presence of the amorphous phase in the microstructure, as shown in Fig. 7. The amorphous phase was not shown in the XRD results due to its small quantity, which may be caused by the evaporation and condensation of the Li compounds.

Table 1 shows the microwave dielectric properties of the typical $Li_{0.774}Zr_{0.057}NbO_3$ ceramics prepared from various calcination and sintering temperatures. The dielectric constants of dense $Li_{0.774}Zr_{0.057}NbO_3$ ceramics are ranging from 28 to 33. It exhibits the same trend as the density, which increases with the sintering temperatures. The $Q \times f$ values of $Li_{0.774}Zr_{0.057}NbO_3$ ceramics are ranging from 3000 to 4500, which have a strong correlation with the grain size, as shown in Fig. 5. This is due to the facts that a larger grain size, derived

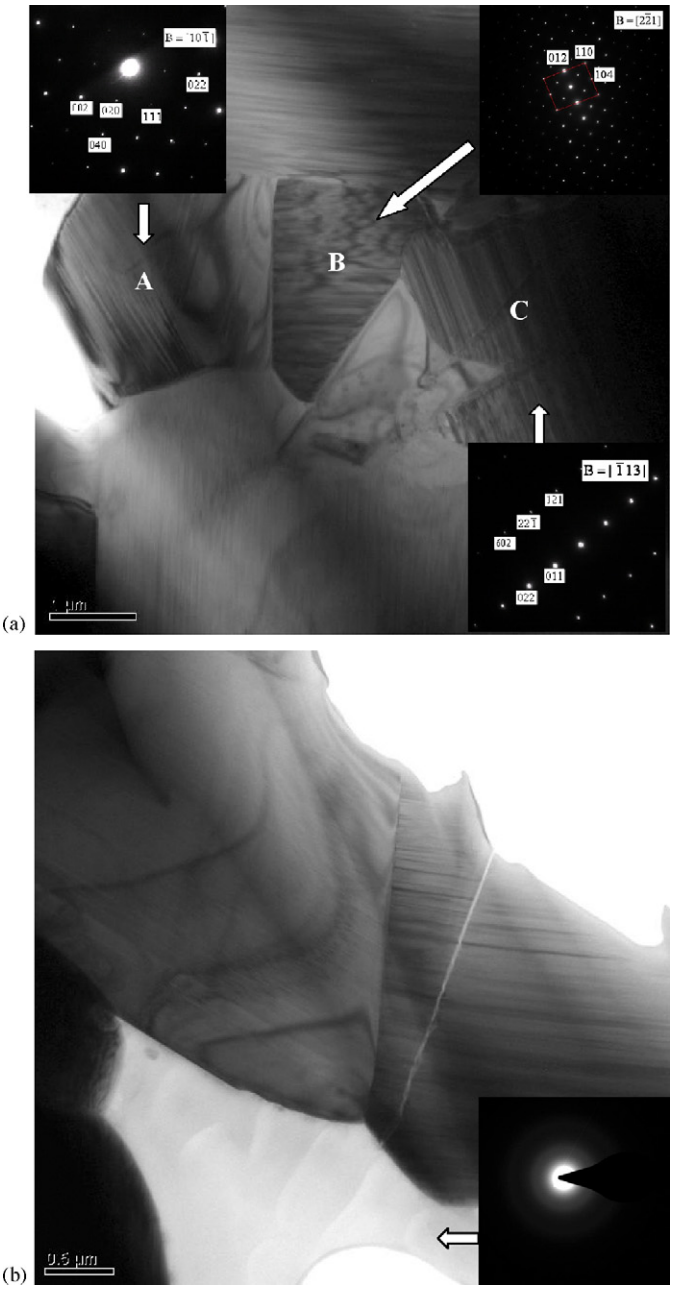

Fig. 7. Transmission electron micrographs of the $Li_{0.774}Zr_{0.057}NbO_3$ ceramics, with calcination temperature at 1150 °C, sintered at 1150 °C: (a) TEM BF image of $Li_{0.774}Zr_{0.057}NbO_3$ ceramics after sintering showing the areas A and B are $Li_{0.774}Zr_{0.057}NbO_3$ phase and area C is $LiNb_3O_8$, and (b) TEM BF image of $Li_{0.774}Zr_{0.057}NbO_3$ ceramics with the existence of amorphous phase.

Table 1
Microwave dielectric properties of $Li_{0.774}Zr_{0.057}NbO_3$ ceramics prepared at different conditions

Calcination temperature (°C)	Sintering temperature (°C)	ε_r	$Q \times f$ (GHz)	τ_f (ppm/°C)
1000	1150	33.01	4463.63	−28.58
1050	1150	27.75	3371.90	−24.79
1100	1150	38.66	2935.80	−16.63
1150	1150	30.97	3551.38	−15.91

from a higher sintering temperature, possesses a better ordering of the ions, which produces the higher $Q \times f$ values. Table 1 also shows that τ_f value is strongly dependent on the calcination temperature. Typically, a higher calcination temperature enabled the temperature coefficient of resonant frequency near zero.

4. Conclusion

The microstructure and the microwave dielectric properties of the new orthorhombic perovskite phase $Li_{0.774}Zr_{0.057}NbO_3$ were investigated. High-density $Li_{0.774}Zr_{0.057}NbO_3$ ceramics (>95% T.D.) can be obtained after sintered at 1150 °C. XRD results show that $Li_{0.774}Zr_{0.057}NbO_3$ phase exists as the main phase with a minor $LiNb_3O_8$ phase, which is confirmed by TEM results. The grain sizes of ceramics sintered at 1150 °C are in the range of 5–9 μm. Typical microwave dielectric properties for dense $Li_{0.774}Zr_{0.057}NbO_3$ ceramics are as followed: $\varepsilon_r \approx 39$, $Q \times f \approx 4500$, and $\tau_f = -16.6$ ppm/°C, measured at 6 GHz. The dielectric constants and $Q \times f$ values of $Li_{0.774}Zr_{0.057}NbO_3$ ceramics have a strong correlation with the density and grain size, respectively.

References

[1] X.H. Zheng, X.M. Chen, Dielectric ceramics with tungsten–bronze structure in the BaO–Nd_2O_3–TiO_2–Nb_2O_5 system, J. Mater. Res. 17 (7) (2002) 1664.
[2] Yebin Xu, Yanyan He, Polymeric precursor synthesis of $Ba_{6-3x}Sm_{8+2x}Ti_{18}O_{54}$ ceramic powder, Ceram. Int. 28 (1) (2002) 75.
[3] G. Wolfram, H.E. Gobel, Existence range, structural and dielectric properties of $Zr_xTi_ySn_zO_4$ ceramics ($x + y + z = 2$), Mater. Res. Bull. 16 (1952) 1455.
[4] C.C. Lee, P. Lin, Effect of glass addition on microwave properties of BaO·La_2O_3·4.7TiO_2, Jpn. J. Appl. Phys. 37 (1998) 6048.
[5] A. Borisevich, P.K. Davies, Microwave dielectric properties of $Li_{1+x-y}M_{1-x-3y}Ti_{x+4y}O_3$ (M = Nb^{5+}, Ta^{5+}) solid solutions, J. Eur. Ceram. Soc. 21 (2001) 1719.
[6] M. valant, D. Suvorov, Processing and dielectric properties of sillenite compounds $Bi_{12}MO_{20-\delta}$ (M = Si, Ge, Ti, Pb, Mn, $B_{1/2}P_{1/2}$), J. Am. Ceram. Soc. 12 (2001) 2900.
[7] M. Udovic, M. Valant, D. Suvorov, Dielectric characterization of ceramics from the TiO_2–TeO_2 system, J. Euro. Ceram. Soc. 21 (2001) 1735.
[8] H. Wang, X. Yao, Structure and dielectric properties of pyrochlore-fluorite biphase ceramics in the Bi_2O_3–ZnO–Nb_2O_5 system, J. Mater. Res. 16 (1) (2001) 83.
[9] M.E. Villafuerte-Castrejon, C. Kuhliger, R. Ovando, I.S. Ronald, R.W. Anthony, New perovskite phases in the systems Li_2O–(Nb_2O_5, Ta_2O_5)–ZrO_2, J. Mater. Chem. 1 (5) (1991) 747.
[10] N.J. Damaskos, B.J. Kelsall, Measuring dielectric constants of low loss materials using a broadband cavity technique, Microw. J. 38 (1995) 140.